International Journal of Hyperthermia

ISSN: 0265-6736 (Print) 1464-5157 (Online) Journal homepage: informahealthcare.com/journals/ihyt20

Optimal power deposition patterns for ideal high temperature therapy/hyperthermia treatments

K.-S. Cheng & R. B. Roemer

To cite this article: K.-S. Cheng & R. B. Roemer (2004) Optimal power deposition patterns for ideal high temperature therapy/hyperthermia treatments, International Journal of Hyperthermia, 20:1, 57-72, DOI: 10.1080/02656730310001611099

To link to this article: https://doi.org/10.1080/02656730310001611099

Published online: 09 Jul 2009.

INT. J. HYPERTHERMIA
VOL. 20, NO. 1 (FEBRUARY 2004), pp. 57–72

Taylor & Francis
healthsciences

Optimal power deposition patterns for ideal high temperature therapy/hyperthermia treatments

K.-S. CHENG and R. B. ROEMER

Department of Mechanical Engineering, 50 S Central Campus Drive, University of Utah, Salt Lake City, UT 84112, USA

(*Received 2 March 2003; revised 6 June 2003; accepted 18 July 2003*)

If it were possible to achieve, an ideal high temperature therapy or hyperthermia treatment would involve a single heating session and yield a desired thermal dose distribution in the tumour that would be attained in the shortest possible treatment time without heating critical normal tissues excessively. Simultaneously achieving all of these goals is impossible in practice, thus requiring trade-offs that allow clinicians to approach more closely some of these ideal goals at the expense of others. To study the basic nature of a subset of these trade-offs, the present simulation study looked at a simple, ideal case in which the tumour is heated by a single, optimized (with respect to space) power pulse, with no power deposition in the normal tissue. Results were obtained for two different clinical strategies (i.e. trade-off approaches), including: (1) an 'aggressive' approach, wherein the desired, uniform thermal dose is completely delivered to the tumour during the power-on period. This approach gives the clinician the satisfaction of knowing that the tumour was treated completely while power was being delivered, and yields the shortest attainable tumour dose delivery time. However, that benefit is attained at the cost of both 'overdosing' the tumour during the subsequent cool down period and, paradoxically, requiring a longer, overall treatment time. Here, the treatment time is considered as that time interval from the initiation of the heating pulse to the time at which the entire tumour has decayed to a specified 'safe' temperature — below 43°C for our calculations. And, (2) a 'conservative' approach is considered, wherein the desired uniform dose is attained at the post-heating time at which the complete tumour cools back down to 'basal' conditions, taken as 4 h in this study. This conservative approach requires less applied power and energy and avoids the 'overdosing' problem, but at the cost of having a tumour dose delivery time that can be significantly longer than the heating pulse duration. This approach can require that clinicians wait a significant time after the power has been turned off before being able to confirm that the desired tumour thermal dose was reached. The present findings show that: (1) for both clinical strategies, an optimal power deposition shape (with respect to position in the tumour) can always be found that provides the desired uniform thermal dose in the tumour, regardless of the heating pulse duration chosen or the tumour perfusion pattern; and (2) shorter heating pulses are preferable to longer ones in that they require less total energy, take less total time to treat the patients, and have optimal power deposition patterns less influenced by perfusion. On the other hand, shorter pulses always require higher temperatures, and for the 'aggressive' clinical approach, they give significantly larger excess thermal doses in the tumour. The aggressive approach always requires longer treatment times than comparable conservative treatments. The optimal power patterns for both strategies involve a high-power density at the tumour boundary, which frequently creates a 'thermal wave' that contributes significantly to the final thermal dose distribution attained.

Key words: Hyperthermia, high temperature therapy, thermal surgery, thermal dose, optimal power deposition, treatment planning.

* To whom correspondence should be addressed. e-mail: roemer@mech.utah.edu

International Journal of Hyperthermia ISSN 0265–6736 print/ISSN 1464–5157 online
http://www.tandf.co.uk/journals
DOI: 10.1080/02656730310001611099

1. Introduction

The clinical potential of high temperature therapy (HTT) has become increasingly promising as additional studies show that it could significantly improve treatments at many important tumour sites (e.g.[1,2]). Despite these encouraging results, there are still major practical concerns involved when applying HTT, including; (1) patient pain, (2) under-dosed targets, (3) long treatment times and (4) normal tissue damage[3–7]. Thus, improved strategies are needed to control optimally the thermal dose delivered in the normal tissues and the tumour.

A fundamental optimization question concerns the geometric shape of the power deposition pattern needed to generate a desired (e.g. uniform) thermal dose in the tumour. For conventional hyperthermia, Ocheltree and Frizzell[8,9] solved a similar problem by determining the optimal patterns needed for generating uniform tumour temperatures. Their work, based primarily on a one-dimensional (1D) model with power deposited only in the tumour (as done in the present study), was useful in guiding other efforts to find optimal power depositions for more complicated conventional hyperthermia problems. The present study extends their work (1) by determining the power deposition patterns that produce a uniform thermal dose (as opposed to a uniform temperature) in the targeted tumour; (2) by considering a range of heating pulse durations, from short time, pulsed heating using the higher powers typical of HTT applications to longer 'pulses' and lower powers — whose limit is the conventional hyperthermia case studied by Ocheltree and Frizzell; and (3) by considering different clinical strategies for reaching the proposed uniform thermal dose in the tumour. Treating tumours to a uniform thermal dose allows one to consider the variety of different time–temperature histories present in pulsed heating with a single metric — as based on the fact that cell death depends on both temperature and time in a form that can be condensed into a single factor, the thermal dose[10,11]. The choice of using the thermal dose as the metric of treatment delivery efficacy is becoming common in both conventional hyperthermia (e.g.[12]) and HTT applications (e.g.[6,7,12–17]). Thermal dose can be used to predict either cell death, microvascular stasis and/or tissue coagulation boundaries depending on the activation energy used in the 'Arrhenius' equation[18].

2. Materials and methods

The following describes the patient, power deposition and thermal models, the numerical method used to solve the thermal model, the objective function that defines the optimal goal and the optimization procedure used to determine the optimal (spatial) distribution of powers. In these initial studies, we would restrict ourselves to the simple, idealized case of a single heating session or 'pulse' to treat the patient, with power deposited only in the tumour. By neglecting the energy deposited outside the tumour, and by considering only a single heating session/pulse, both of which have the effect of neglecting the time needed to allow for normal tissue cooling that is required in a real treatment, this idealized power deposition model approach provides a limiting 'best case' analysis[19] that results in the shortest possible treatment times. That is, adding normal tissue heating and multiple pulses, e.g. for large solid tumours, and the additional waiting periods between pulses, will result in even longer treatment times. It was found that even given these idealizations, clinical trade-offs must be made in determining the 'optimal' power depositions to be applied. This simple modelling approach can give insights into the limits of, and the basic nature of, the trade-offs required in more practical situations.

Table 1. Physiological parameters

Tissue density (ρ, kg/m^3)	Tissue and blood specific heat (C_p and C_b, J/kg/°C)	Tissue thermal conductivity (k, W/m/°C)	Pennes' perfusion parameter (W_b, kg/m^3/s)	Arterial blood temperature (T_b, °C)
1000	3770	0.55	0.0, 0.25, 0.50, 0.75, 1.0, 5.0, 10.0	37

2.1. *Patient, power and thermal models*

The study used a simplified 1D Pennes Bio-Heat Transfer Equation (BHTE) model[20]:

$$\rho \cdot C_p \cdot \frac{\partial T}{\partial t} = k \cdot \frac{\partial^2 T}{\partial x^2} - W_b \cdot C_b \cdot (T - T_b) + Q. \tag{1}$$

The idealized patient generally has the homogeneous properties as listed in table 1 — with the exception of one case where the tumour perfusion varied with position. The tissue model consisted of (1) normal tissue that extended from $x = 0$ to the left margin of the tumour at $x = 5.1$ cm and (2) 'the tumour', which extended from that location to the tumour centreline at $x = 7.5$ cm. (The tumour and normal tissue geometry were symmetrical about that centreline.) The boundary conditions used were a temperature of 37°C at $x = 0$, and zero heat flux at the tumour centreline. Owing to the symmetrical geometry being modelled, we only need to calculate temperatures in the left half domain when the right (centreline) boundary condition was given as the no flux boundary condition. Inside the tumour, the power density could vary with position, with eight independent power density magnitudes (preliminary tests[21] found that eight independent magnitudes were sufficient to reach a uniform thermal dose distribution in one side of the symmetric tumour model). The widths of the eight uniform power density deposition regions were each 3 mm, and the power within each of these eight regions remained constant for the duration of each heating pulse. No power was deposited in the normal tissue. Both homogeneous and heterogeneous perfusion distributions were studied (the seven homogeneous perfusions are given in table 1; the heterogeneous distribution is given in figure 9a).

2.2. *Numerical model*

The solution of equation (1) was obtained using the Crank–Nicholson finite difference method[22]. All computations were carried using an initial condition of 37°C, a time step of 0.1 s and a spatial interval of 3 mm. The thermal dose was evaluated using a widely accepted empirical Sapareto–Dewey formula (equation 2;[10,11]). To ensure that the whole domain cooled down to basal conditions for all cases,[21] the duration for computing the total thermal dose accumulated was chosen as 4 h. The numerical evaluation of the thermal dose used the midpoint rectangular quadrature rule[23] and $T_{\text{ref}} = 43$°C:

$$\text{TD} = \int_0^{t_T} R^{T - T_{\text{ref}}} \cdot \mathrm{d}t, \quad \text{where} \begin{cases} R = 2, & \text{for } T \geq T_{\text{ref}} \\ R = 4, & \text{for } T < T_{\text{ref}} \end{cases} \tag{2}$$

2.3. *Optimization approach*

The objective function that was minimized (equation 3) was the averaged sum over all finite difference nodes in the tumour of the squares of the normalized differences between the calculated and ideal thermal doses. This was equivalent to minimizing the tumour's normalized thermal dose's variance:

$$J = \frac{1}{n_x} \cdot \sum_{\text{tumour region}} \left(\frac{\text{TD}(x)_{\text{calculated}}}{\text{TD}_{\text{desired}}} - 1 \right)^2. \tag{3}$$

For these studies, the desired thermal dose was set at 245 cumulative equivalent minutes at 43°C (245 CEM43°C), a value close to that used by several other investigators (e.g.[24,25]). Our simulations were performed for two primary clinical strategies, an 'aggressive' protocol in which the uniform thermal dose was achieved immediately at the end of the heating period, and a 'conservative' protocol for which the desired uniform thermal dose was reached at the end of the 4 h. We also studied a few 'intermediate' protocol cases for which the uniform thermal dose was delivered at a time between the end of the heating period and the end of the 4 h. The variable metric algorithm, one of the Newton's method family[26], was used to determine the optimal power deposition magnitudes for each heating duration case, i.e. to determine the eight power amplitudes that gave a uniform thermal dose in the tumour at the end of the desired 'tumour dose delivery time'. These optimal distributions were determined for power-on (heating session or 'pulse') durations of 5, 10, 20, 40 s, 1, 2, 4, 5, 10, 20, 40 min, 1, 2, 2.5 and 3 h to determine how the power-on duration influenced the results.

Specific results evaluated included the distributions of optimal power deposition magnitudes inside the tumour, the peak power magnitudes and total energy delivered during the heating period and the length of the treatment time. Initially, one might be tempted to take the 'treatment time' as either the power-on time (which would make both the aggressive and conservative approaches have the same treatment times), or the time at which the desired thermal dose was reached in the tumour, i.e. the tumour dose delivery time (which would give the maximum time difference between these two strategies). Clinically, however, for both strategies (but more significantly for the aggressive strategy) (1) the tumour temperatures were significantly elevated above 43°C at the end of the heating period, particularly for short pulses, and thus (2) a significant thermal dose could be accrued by the patient after the power was turned off. In some cases, this additional thermal dose could put the patients at risk, e.g. for vascular damage and bleeding in the tumour, and/or the heated normal tissues after the power was turned off[27,28]. In cases where this was of clinical concern, the patients would need to remain in the magnetic resonance imaging (MRI) system for observation until all temperatures decayed to some acceptable level. Damage to critical vascular structures can be very serious, and since it has been shown that the thermal dose approach can give good predictions of tissue damage[3,27,28], waiting for all of the temperatures to decay below a certain value (e.g. 43°C) would constitute a safe clinical procedure. To account for this, treatment time was considered as the time interval starting from the initiation of the heating pulse to the time at which the entire tumour had decayed to a specified 'safe' temperature, 43°C for our calculations.

3. Results

First, to illustrate both (1) that the desired uniform thermal doses can indeed be delivered by optimizing the eight power magnitudes, and (2) how the optimized thermal dose patterns evolve in time, figure 1 shows the 'conservative' strategy thermal dose (TD) distributions for a uniform perfusion of 0.5 kg/m^3/s for three different heating pulse durations. The results are shown both at the end of each heating pulse, and at the end of 4 h when the tumour is uniformly dosed. To illustrate the power deposition patterns needed to obtain these uniform thermal doses for the 'conservative' approach, figure 2 shows the optimal distributions of the eight power magnitudes for nine cases (three different pulse durations and three different perfusion magnitudes). Figure 3 shows an important phenomenon observed with short pulse durations, i.e. there is initially a peak temperature at the tumour boundary, which moves inwards after power is turned off. This peak temperature and the associated 'post-heating thermal wave' can provide a significant fraction of the desired thermal dose. For example, for the 5-s power-on duration case, while the TD on the tumour boundary is approximately 15 CEM43°C at 5 s (figure 1), it rapidly accumulates to become about 219 CEM43°C at 55 s.

For the aggressive strategy, figure 4 shows the optimal power density distributions for the same nine cases as used in figure 2 for the conservative approach. To illustrate the cost of the trade-offs associated with the aggressive strategy,

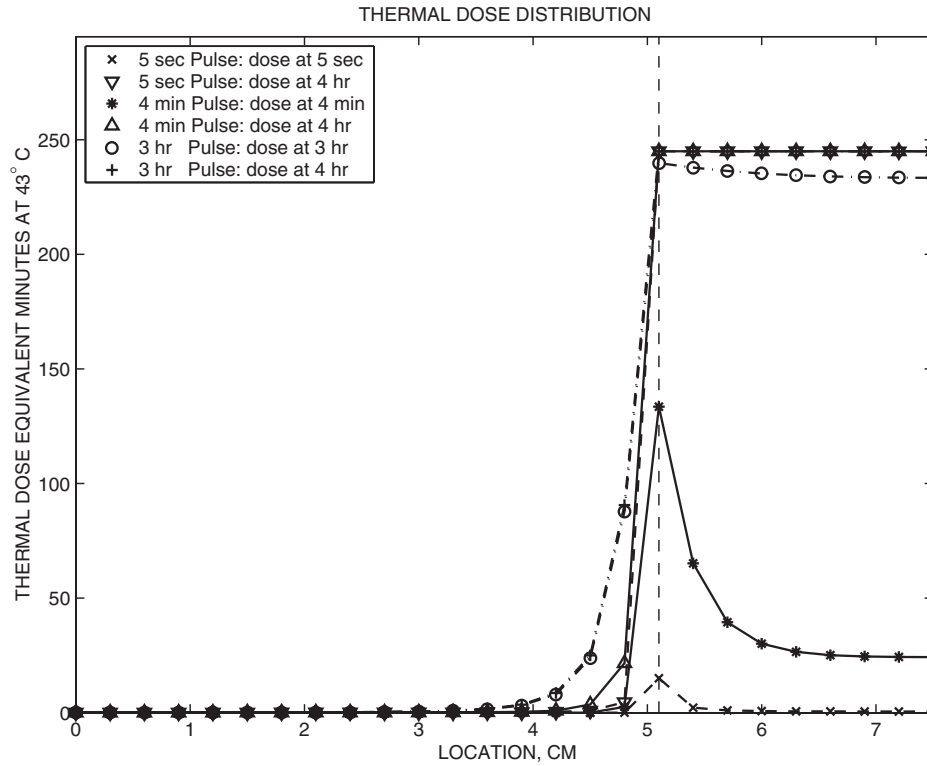

Figure 1. Thermal dose distribution at the end of the power-on period and at the end of 4 h for the power-on durations of 5 s, 4 min and 3 h for the 'conservative' strategy at a 0.50 kg/m^3/s perfusion value.

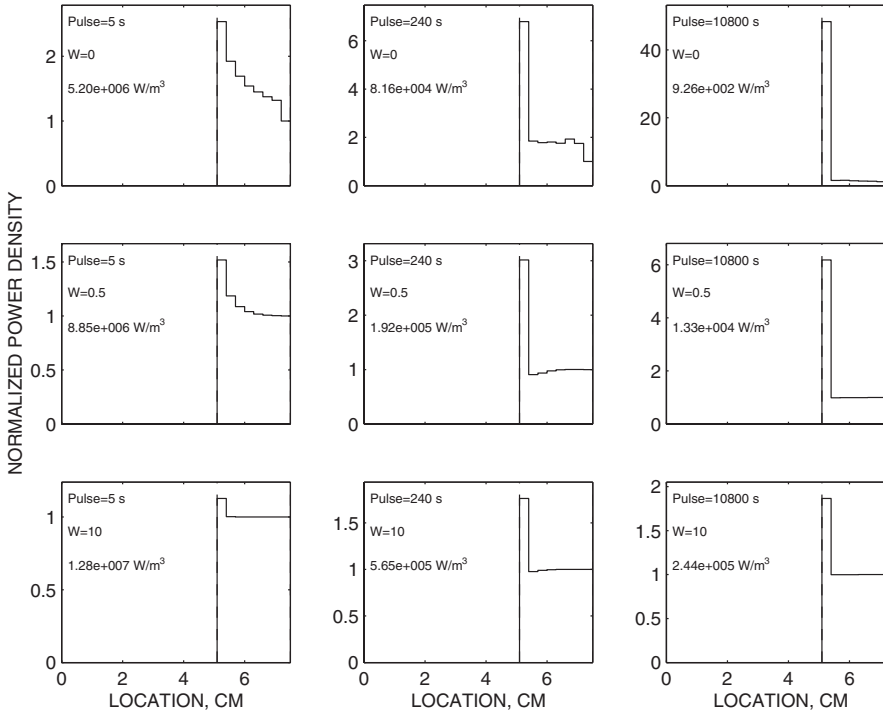

Figure 2. Optimized, conservative strategy power patterns (normalized to the tumour centre) needed to generate a uniform thermal dose in the tumour. The columns show the results for three different pulse durations, while the rows show results for three different (uniform) perfusions. The non-dimensional numbers in the graphs give the power densities at the tumour centre. Note the large-scale changes among the graphs.

figure 5 shows the maximum (over all tumour locations) excess thermal dose in the tumour as a function of the heating time, for several different (uniform) blood perfusion magnitudes.

To illustrate the effect of perfusion magnitude, figure 6 compares the maximum power and the total absorbed energy in the tumour (the summation of all eight powers integrated over the heating time) for different heating pulse durations and uniform perfusions for both clinical heating protocols.

To evaluate the differences in the temperatures required to obtain optimal thermal doses for the two different clinical protocols, figure 7 shows the maximum temperature in the tumour at the time when power is just being turned off and the associated standard deviations of the temperatures in the tumour at that time for the two protocols.

Figure 8 summarizes the variations of the 'treatment time' (the time required for every point in the tumour to decay below 43°C) for both clinical protocols.

Figure 9 gives the heterogeneous perfusion settings used to evaluate the ability of this approach to optimize the power deposition pattern for non-uniform perfusion patterns. This perfusion pattern follows that determined by Toglia *et al.*[29] for *in vivo* human glioblastoma multiforme.

To study the effects of different 'intermediate' protocols, figure 10 presents results for a 5-s heating period, for both the conservative and aggressive strategies, and for three 'intermediate' strategies where the uniform thermal dose is reached at

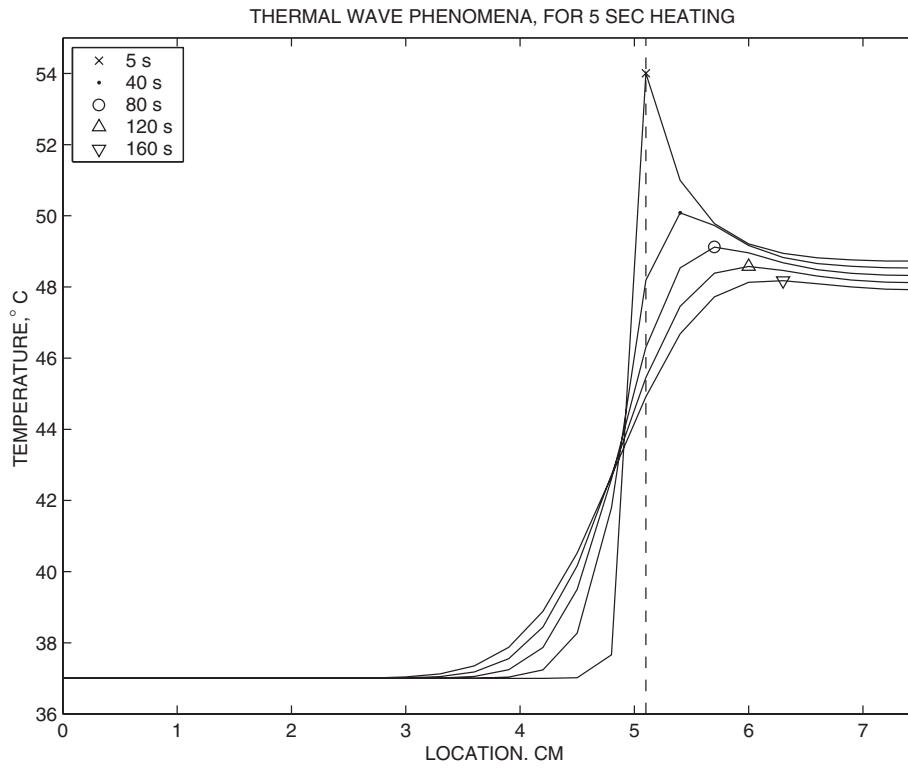

Figure 3. 'Thermal wave' changing with time for a perfusion of 0.50 kg/m^3/s and a 5-s heating period in a 'conservative' heating approach (see figures 1 and 2).

intermediate dose delivery times of 10 s, 2 and 10 min. Presented are the temperature distributions at the end of power on, the optimized power deposition patterns and the thermal dose distributions at 4 h for a uniform 0.50 kg/m^3/s perfusion.

Finally, figure 11 shows the effects of using different intermediate dose delivery times for a perfusion of 0.5 kg/m^3/s. Curves for six different heating times are given to show how the maximal excess thermal dose and the peak temperature at the end of power-on, change with the intermediate dose delivery time.

4. Discussion

As with Ocheltree and Frizzell's results[8,9], several important, basic observations can be drawn from the results of this idealized 1D study and generalized to guide future, more realistic research efforts, in particular regarding the optimal power deposition patterns. Most basically, it is clear that if the tumour perfusion is known, an optimal power deposition pattern can always be found (i.e. for any desired heating time) that produces a uniform tumour thermal dose at a time specified by the clinician, e.g. at the end of the power-on period for the aggressive strategy (figure 5), at the time when the complete tumour has reached basal conditions for the conservative strategy (figure 2), or at any desired intermediate dose delivery time (figure 10). These optimal power deposition patterns are influenced by the user's choice of the power-on period and clinical strategy, and by the magnitude/distribution of the blood perfusion. Similar to the conventional

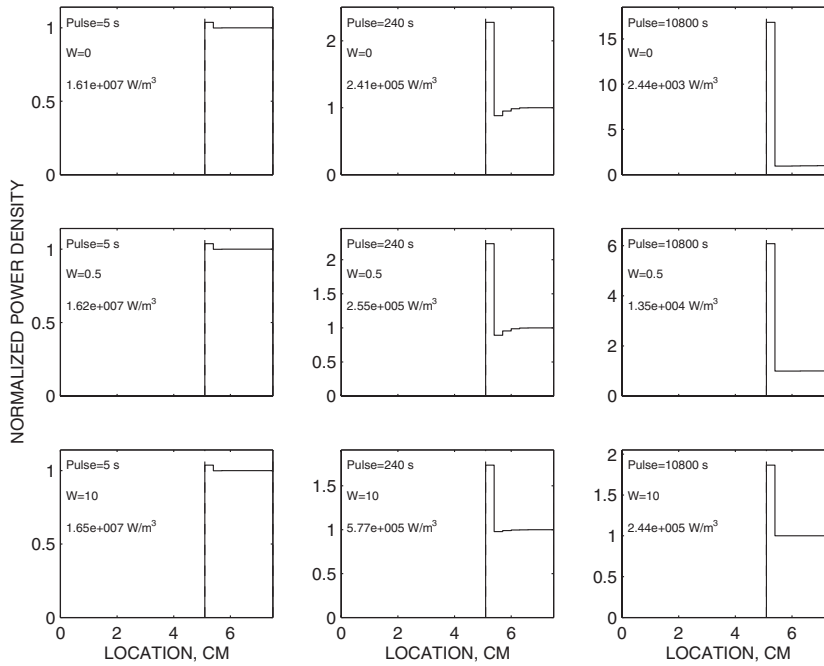

Figure 4. Aggressive strategy's normalized power deposition patterns (again normalized to the tumour centre) needed to generate a uniform thermal dose in the tumour, for the same pulse durations and perfusions as for the 'conservative' approach in figure 2.

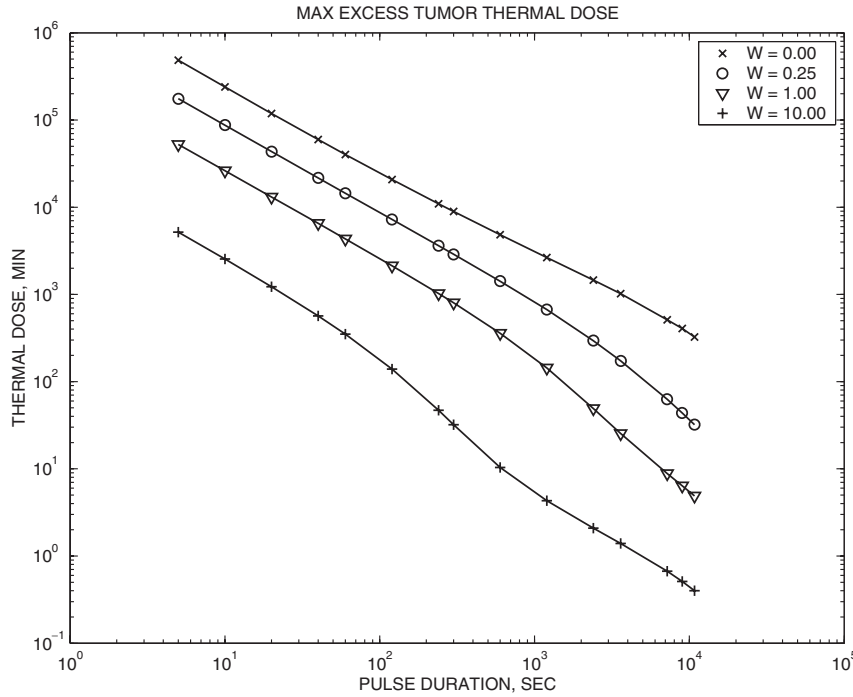

Figure 5. Maximal excess thermal dose (above 245 CEM43°C) in the tumour versus the heating pulse duration for several perfusions for the aggressive protocol.

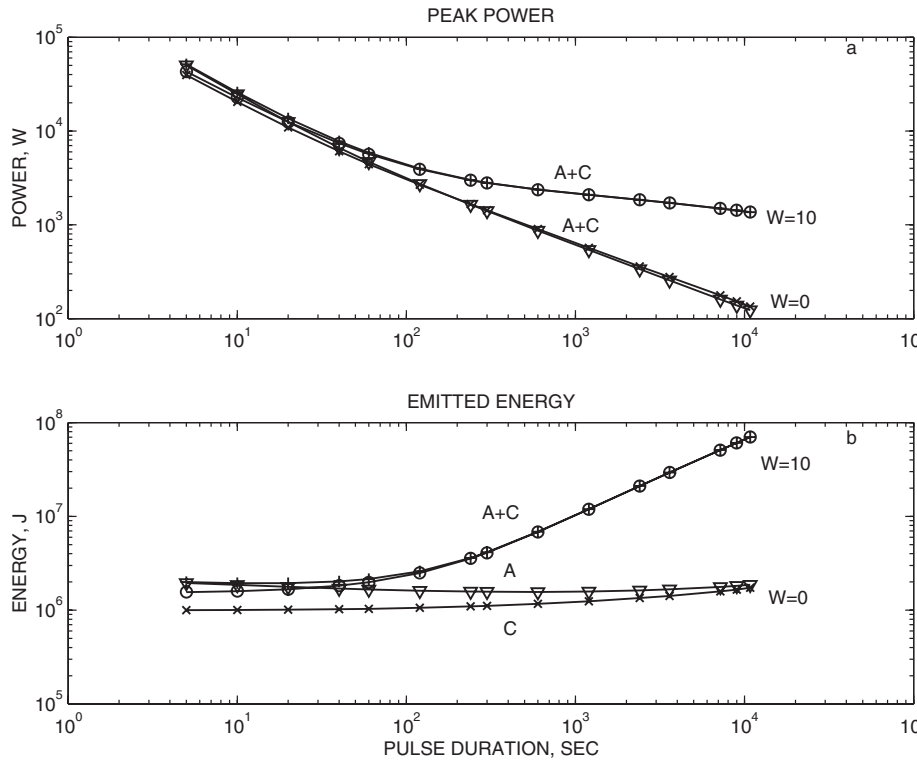

Figure 6. Peak power and total energy delivered for two perfusions for both the aggressive (A: + ▽) and conservative (C: × and ○) clinical approaches.

hyperthermia results of Ocheltree and Frizzell for the uniform temperature case, all of the current uniform tumour thermal dose (UTTD) studies show that a maximum in power deposition must occur at the tumour boundary to compensate for the conduction cooling to the surrounding tissues — as was also seen by Wan *et al.*[30] for a set of 'intermediate' optimal power deposition cases using Gaussian temperature profile approximations. What is different for the UTTD is that the magnitudes of the power densities are not always monotonically decreasing functions of position from the tumour boundary to the tumour centre. That is, for some intermediate heating durations, the power densities show a 'dip' adjacent to the tumour edge and then gradually increase toward the tumour centre for both protocols (see the middle columns of figures 2 and 4). This difference arises since in the UTTD cases the peak power at the tumour boundary plays an additional role (beyond overcoming boundary conduction) of creating a thermal wave that provides a significant part of the thermal dose in the tumour interior. That is, it also serves as an 'energy source' for generating the UTTD. The 'dip' is needed to compensate for the effects of the 'thermal wave' moving inwards. These inward moving waves will be equally significant in determining the optimal power deposition patterns for, and the relative timing of, multiple pulses needed to heat large, three-dimensional (3D) tumours with more realistic power deposition patterns that include normal tissue heating. Those optimal power patterns will consist of a series of optimally superimposed thermal waves produced in different required locations/times.

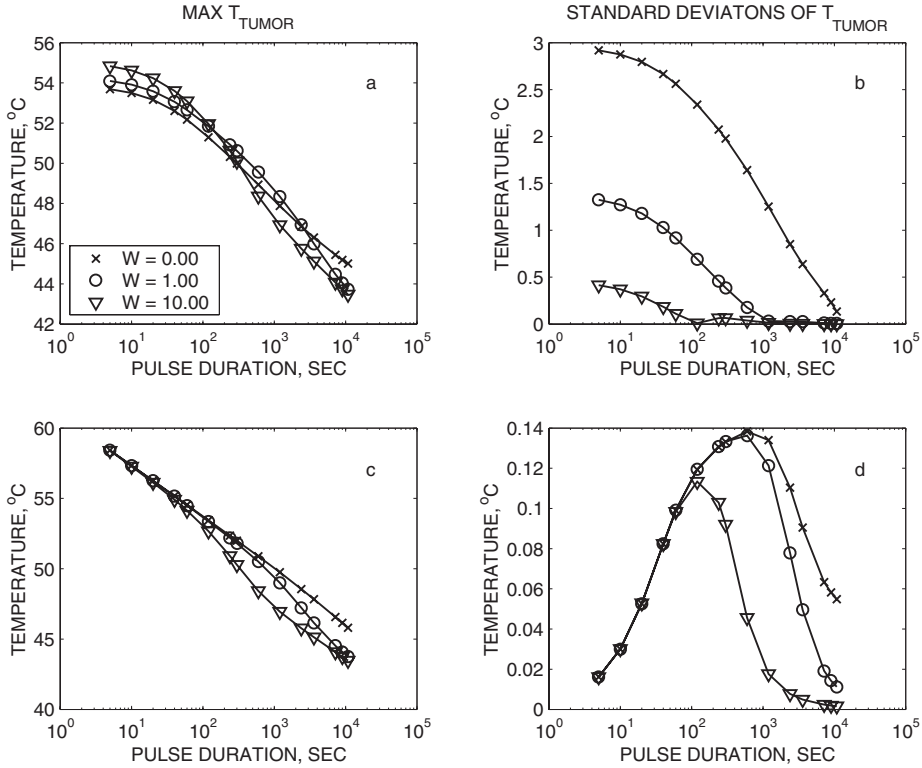

Figure 7. Maximum tumour temperatures and standard deviations of the tumour temperatures at the end of the heating pulse for different pulse durations and perfusions for the conservative (top row) and aggressive (bottom row) protocols. Note the scale changes among the graphs.

Indeed, the remaining characteristics of the optimal power deposition shapes can be best explained in terms of the 'thermal waves' that are created by the boundary power peaks. That is, for both strategies (figures 2 and 4), (1) the relative magnitudes of these peaks get smaller as the perfusion level increases (for a fixed heating time). This occurs since the higher the perfusion level is, the harder it is for the thermal wave to penetrate into the interior of the tumour since the high temperatures in the thermal wave are convected away more rapidly at higher perfusions. Thus, as perfusion increases, not only does the total amount of power-required increase, but the more central zones require higher fractions of that total in order to be optimally treated. (2) As the heating pulse duration increases, not only does the maximum power required decrease (since the required energy is now delivered over a longer period), but this also reduces the boundary temperatures and thus the size of any thermal wave present. However, the relative peak powers at the tumour boundary for the aggressive strategy are always smaller than those for the conservative strategy, since the aggressive strategy requires more power at every point in the tumour to reach the specified UTTD at the time when power is turned off. The increased temperature values associated with these increased powers take time to decay, thus resulting in the excess thermal doses in the tumour. As expected, the excess thermal doses get larger when the perfusion decreases since the temperatures decay

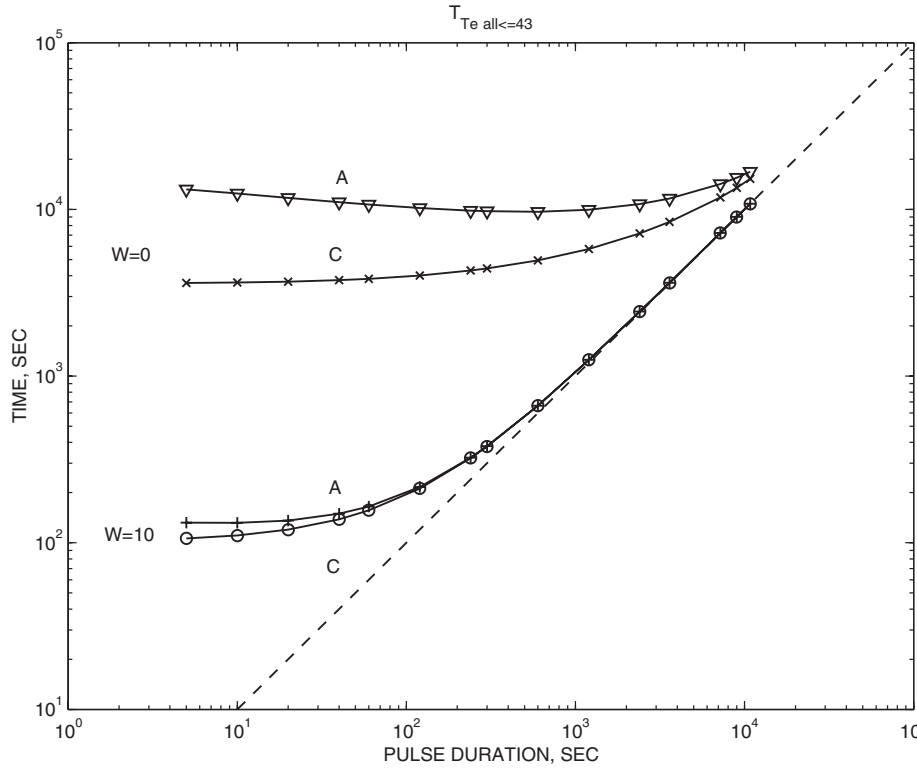

Figure 8. Variation in the 'treatment time', i.e. the time required for every point in the tumour to decay below 43°C ($t_{\mathrm{Te\ all}\leq 43}$) for the conservative (C) and aggressive (A) clinical strategies. The curves shown denote how these critical times change with the heating pulse period for a high and a low uniform perfusion value.

more slowly, and smaller when the heating pulse duration increases since the peak temperatures are lower. The resulting excess thermal doses can possibly cause vascular damage and bleeding[18], and they thus may require longer 'treatment times' to observe the patient when large vessels traverse the tumour and/or critical normal tissues are being heated.

The peak powers required to achieve these UTTDs (figure 6) vary little with strategy choice, however. The fact that both strategies require close to the same peak power for any given blood flow is due to (1) the strong non-linear temperature/dose relationship, for which a small change in peak temperature (needing only small change in power) gives a large change in thermal dose, and (2) since a significant amount of power is required to overcome boundary conduction effects in all cases, thus the peak power (which always occurs at the tumour boundary) is only partially determined by blood perfusion. Thus, while the aggressive strategy will always have higher power and temperatures than the conservative approach (compare figures 2 and 4) they do not need to be much higher, thus explaining figure 6a (and figure 7a, c). Similarly (figure 6b), the aggressive strategy requires a somewhat larger total applied energy — which results in the excess thermal dose — than does the conservative approach, with larger perfusions and heating times requiring increased total energy depositions. In clinical applications, these increased

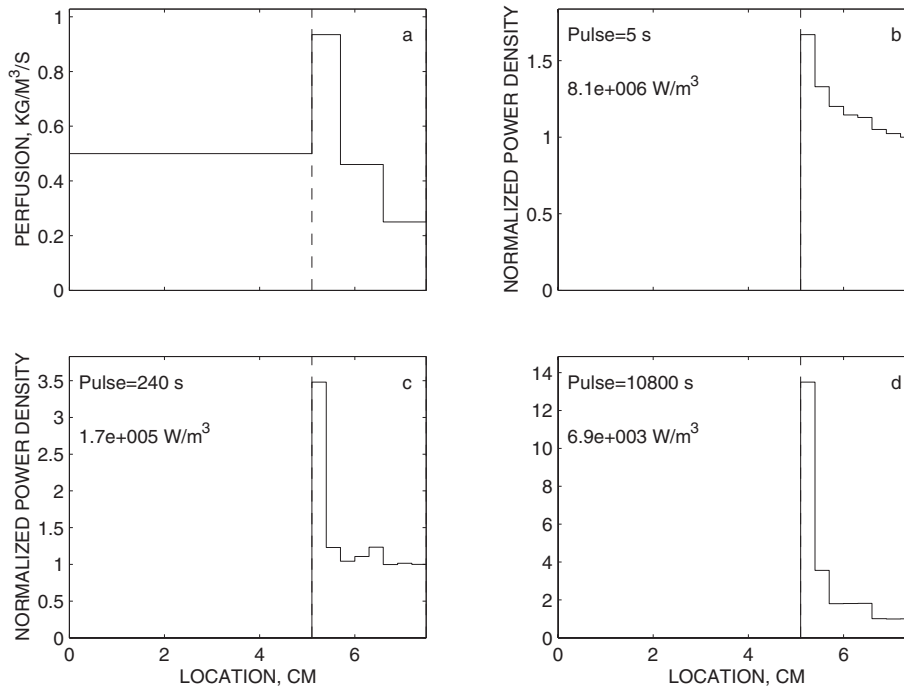

Figure 9. (a) Heterogeneous perfusion distribution used in these simulations; (b–d) resulting optimal power deposition patterns for different heating periods for the conservative protocol, again normalized to the centreline.

tumour energy depositions would have associated increased energy deposition in normal tissues, with the possible attendant normal tissue complications.

Next, figure 8 shows that the additional energy deposited by the aggressive strategy could have a second undesirable effect, that is increasing the 'treatment time', if one defines that as the time required for the patient's tumour to decrease to a prescribed, acceptable temperature — 43°C in our studies. Part of these increased delays is due to the higher overall powers required by the aggressive approach, and part by the movement of the thermal waves inward which cause the temperatures in the tumour to decay more slowly. These factors result in a (paradoxically) longer overall treatment time for the aggressive approach than is needed for a comparative conservative case. In addition, these results show that for these ideal treatments, the aggressive therapy treatment times are more sensitive to blood flow variations than the conservative treatments — for a fixed heating pulse duration. Thus, while many investigators have pointed out the potential advantages of short time, HTT applications in terms of their being less dependent on perfusion (when compared to conventional hyperthermia), this particular result (treatment time as defined above) shows the opposite trend.

As shown in figure 9, the optimal power deposition pattern becomes more dependent on the perfusion pattern as the power-on period increases, and eventually reaches the same pattern as predicted by Ocheltree and Frizzell for very long heating periods, as expected. Also by comparing the $W = 0.5\,\mathrm{kg/m^3/s}$ results in figure 2 for a homogeneous perfusion and the heterogeneous results (but with an average tumour

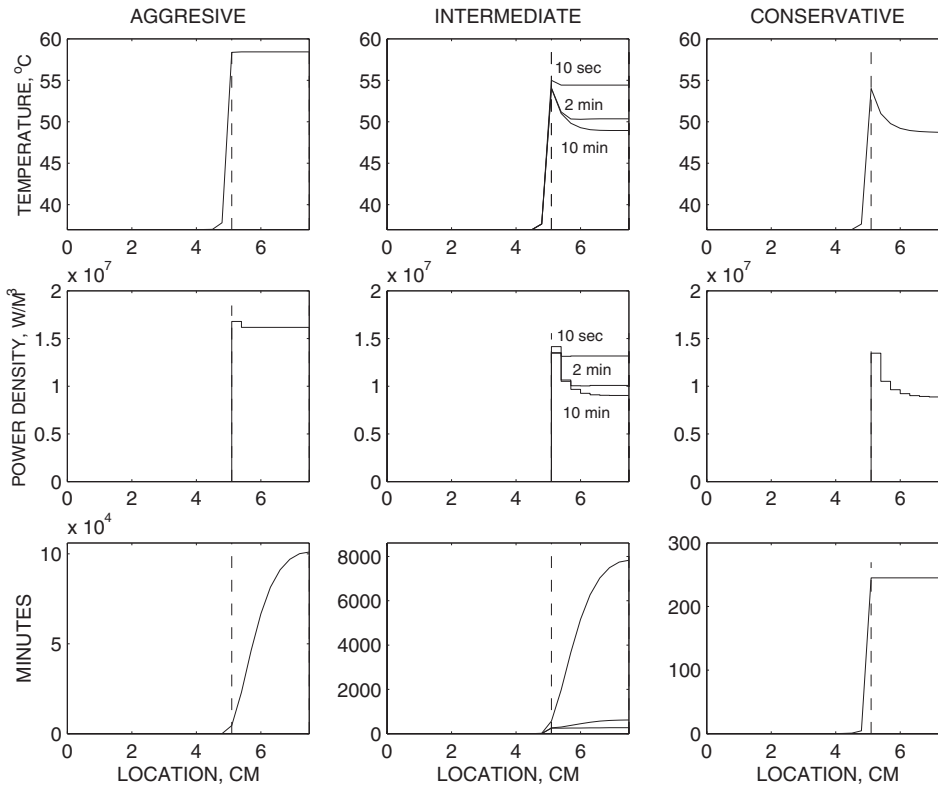

Figure 10. Temperature distribution at the end of the power-on period, the optimal power deposition pattern and the thermal dose distribution at the end of 4 h for five controlled times at which the tumour reaches a uniform thermal dose level of 245CEM43°C (5 s, aggressive approach; 10 s, 2 and 10 min, intermediate approach; 4 h, conservative approach) for a 5-s heating period and a 0.50 $kg/m^3/s$ perfusion.

perfusion of $W = 0.5\,kg/m^3/s$) in figure 9 for comparable heating times, one can clearly see that at short heating times, the homogenous and heterogeneous results are very similar, but for longer heating times they diverge, which reflects the fact that the perfusion is taking out more energy at longer heating time periods[31].

Figures 10 and 11 show the consequences of choosing thermal dose delivery times that fall between the aggressive and conservative strategies for a uniform perfusion of 0.5 $kg/m^3/s$. For example, one might want to choose an intermediate strategy so that a maximum tumour temperature was not exceeded. From figure 11, when one chooses a lower peak temperature, one is still free to choose a range of intermediate treatment protocols, i.e. various combinations of the power-on period and the dose delivery time. It is also clear that there is a lower temperature limit that must be reached to obtain the desired thermal dose for a given power-on period.

5. Summary

In summary, optimal power density patterns can always be found for any perfusion pattern, desired heating time and clinical strategy. For the aggressive approach, shorter heating pulses result in high excess thermal doses in the tumour and require longer treatment times — which in turn are more sensitive to perfusion magnitude

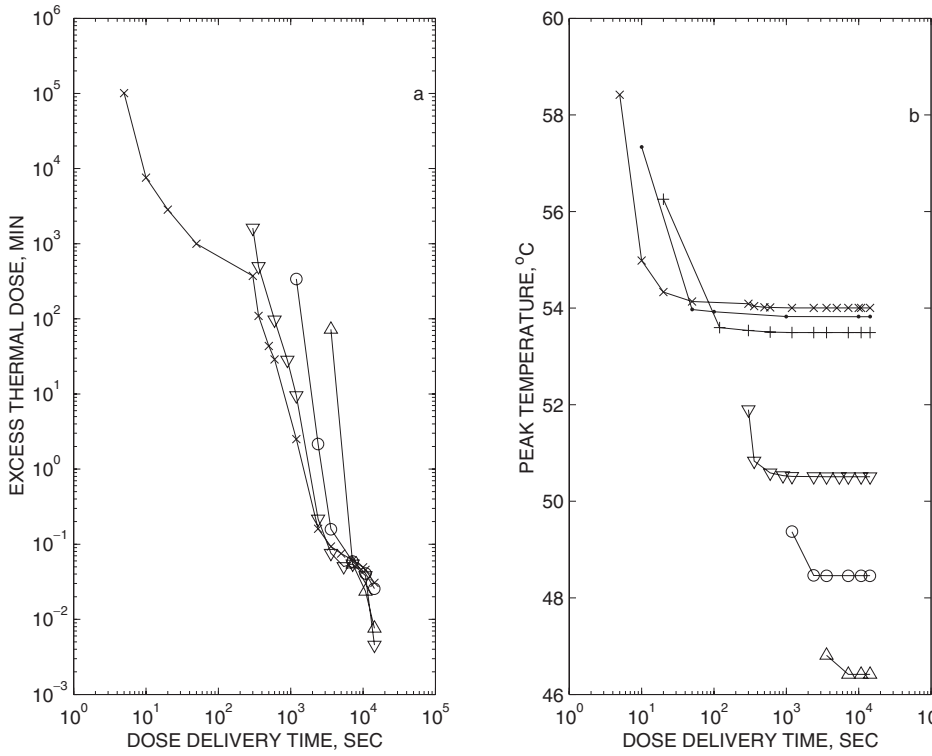

Figure 11. 'Intermediate' strategy results lying between the aggressive and conserve strategy results for a perfusion of 0.50 kg/m^3/s. The top left-hand point of each curve represents the aggressive strategy, while the lower right-hand point represents the conservative approach. The heating pulse durations are used were: 5 (×), 10 (●), 20 (+), 300 (▽), 1200 (o) and 3600 (△) s. The controlled dose delivery times ranged from 5 to 14 400 s. The peak temperatures occurred at the end of the heating pulses.

than are the corresponding conservative treatments. The 'thermal waves' created by the need for increased boundary heating in the optimal cases studied here contribute significantly to (1) the achievement of the optimal dose distribution in the conservative approach and (2) the undesirable excess thermal doses in the tumour interior in the aggressive approach.

The optimal power deposition shapes found from this idealized 1D study can be used (1) to guide efforts to investigate the clinical trade-offs and (2) to find more efficient computationally feasible, optimal power deposition patterns for more complex 3D cases. For example, it can be clearly inferred from these studies that the optimal heating patterns for 3D tumours heated with multiple pulses in which normal tissue is also heated, will involve the application of multiple, interacting 'thermal waves'. In patients, one would expect that the optimal 3D power deposition patterns would involve the highest power densities at the tumours' 'corners', the second highest at the tumours' edges, and gradually decaying magnitudes toward the tumour centre — with appropriate modifications for variations in blood flow. Pretreatment knowledge of blood perfusion distributions will be essential for finding optimal power patterns in clinical applications, knowledge that can be obtained through the use of MRI or computed topography (CT) technologies[32,33].

Finally, if those pretreatment values change significantly during treatments, something not generally seen in tumours for conventional hyperthermia[34], then model-based feedback control mechanisms can provide compensation (e.g.[35]).

The extensions of these results to determine the optimal power deposition patterns in realistic cases have the potential significantly to improve the application of HTT techniques by eliminating tumour under- and over-dosing, reducing treatment times and the related expenses, and reducing normal tissue pain and damage. The eventual clinical implementation of the basic concepts developed herein will, of course, require considerable further development, including extensions that consider not only more realistic 3D anatomies, blood flow patterns and power deposition patterns, but also multiple pulses and normal tissue heating. We are currently pursuing additional studies that include the above extensions of the current ideal cases, including more extensive studies of the 'thermal wave' phenomena and of the optimal sequence of high focal zone locations for treatments involving multiple high intensity focused ultrasound pulses.

Acknowledgements

Work was supported by NCI Grants RO1 CA33922 and CA87785.

References

1. Schatzl G, Madersbacher S, Djavan B, Lang T, Marberger M. Two-year results of transurethral resection of the prostate versus four 'less invasive' treatment options. *Eur Urol* 2000; 37: 695–701.
2. Burgess SEP, Silverman RH, Coleman DJ, Yablonski ME, Lizzi FL, Driller J, Rosado A, Dennis PH Jr. Treatment of glaucoma with high-intensity ultrasound. *Ophthalmology* 1986; 93: 831–8.
3. Damianou C, Hynynen, K. Focal spacing and near-field heating during pulsed high temperature ultrasound therapy. *Ultrasound Med Biol* 1993; 19: 777–87.
4. Hynynen K. The threshold for thermally significant cavitation in dog's thigh muscle *in vivo*. *Ultrasound Med Biol* 1991; 17: 157–69.
5. Fan X, Hynynen K. Ultrasound surgery using multiple sonications — treatment time considerations. *Ultrasound Med Biol* 1996; 22: 471–82.
6. Hazle J, Diederich C, Kangasniemi M, Price R, Olsson L, Stafford R. MRI-guided thermal therapy of transplanted tumors in the canine prostate using directional transuretharal ultrasound applicator. *J Magn Res Imag* 2002; 15: 409–17.
7. Hynynen K, Pomeroy O, Smith DN, Huber PE, McDannold NJ, Kettenbach J, Baum J, Singer S, Joiesz FA. MR imaging-guided focused ultrasound surgery of fibroadenomas in the breast: a feasibility study. *Radiology* 2001; 219: 176–85.
8. Ocheltree KB, Frizzell LA. Determination of power deposition patterns for localized hyperthermia: a steady-state analysis. *Int J Hyperthermia* 1987; 3: 269–79.
9. Ocheltree KB, Frizzell LA. Determination of power deposition patterns for localized hyperthermia: a transient analysis. *Int J Hyperthermia* 1988; 4: 281–96.
10. Sapareto SA, Dewey WC. Thermal dose determination in cancer therapy. *Int J Radiation Oncology Biol Phys* 1984; 10: 787–800.
11. Dewey D, Hopwood L, Sapareto S, Gerwecki L. Cellular response to combinations of hyperthermia and radiation. *Radiology* 1977; 23: 463–74.
12. Hunt JW, Lalonde R, Ginsberg H, Unchuk S, Worthington A. Rapid heating: critical theoretical assessment of thermal gradients found in hyperthermia treatments. *Int J Hyperthermia* 1991; 7: 703–18.
13. Beerlage HP, Thuroff S, Madersbacher S, Zlotta AR, Aus G, de Reijke TM, de la Rosette JJ. Current status of minimally invasive treatment options for localized prostate carcinoma. *Eur Urol* 2000; 37: 2–13.
14. Vallancien G, Chartier-Kastler E, Harouni M, Chopin D, Bougaran J. Focused extracorporeal pyrotherapy: feasibility study in man. *J Endourol* 1992; 6: 173–81.

15. Daum DR, Smith NB, King R, Hynynen K. *In vivo* demonstration of noninvasive thermal surgery of the liver and kidney using an ultrasonic phased array. *Ultrasound Med Biol* 1999; 25: 1087–98.
16. Frizzell LA. Threshold dosages for damage to mammalian liver by high intensity focused ultrasound. *IEEE Trans Ultrason Ferroelec Freq Contr* 1998; 35: 578–81.
17. Loulou T, Scott EP. Optimization of heat treatment in high focused intensity ultrasound treatments. In: Congress Français de Thermique, SFT 2000 Lyon, 15–17 May 2000.
18. Sherar M, Moriarty J, Kolios M, Chen J, Peters R, Ang L, Hinks RS, Hinkelman RH, Bronskill MJ, Kucharcyk W. Comparison of thermal damage calculated using magnetic resonance thermometry, with magnetic resonance imaging post-treatment and histology, after interstitial microwave thermal therapy of rabbit brain. *Phys Med Biol* 2000; 45: 3563–76.
19. Roemer RB, Cetas TC, Oleson JR, Halac S, Matloubieh AY. Comparative evaluation of hyperthermia heating modalities — I. Numerical analysis of thermal dosimetry bracketing cases. *Rad Res* 1984; 100: 450–72.
20. Pennes HH. Analysis of tissue and arterial blood temperatures in the resting human forearm. *J Appl Physiol* 1948; 1: 93–122.
21. Cheng K-S. Optimizing power deposition in arbitrary tumor volumes for ultrasound hyperthermia. PhD dissertation, University of Utah, Salt Lake City, 2003 (expected completion 2004).
22. Press WH, Teukolsky SA, Vetterling WT, Flannery BP. Initial value problems in multi-dimensions. In: *The Numerical Recipes in FORTRAN, The Art of Scientific Computing*, New York: Cambridge University Press, 1992: 844–8.
23. Press WH, Teukolsky SA, Vetterling WT, Flannery BP. Integration of functions. In: *The Numerical Recipes in FORTRAN, The Art of Scientific Computing*, New York: Cambridge University Press, 1992: 130–4.
24. Daum DR, Hynynen K. Thermal dose optimization via temporal switching in ultrasound surgery. *IEEE Trans Ultrason Ferroelec Freq Contr* 1998; 45: 208–15.
25. Fan X, Hynynen K. Control of the necrosed tissue volume during noninvasive ultrasound surgery using a 16-element phased array. *Med Phys* 1995; 22: 297–306.
26. Press WH, Teukolsky SA, Vetterling WT, Flannery BP. Minimization or maximization of functions. In: *The Numerical Recipes in FORTRAN, The Art of Scientific Computing*, New York: Cambridge University Press, 1992: 418–23.
27. Hoogeveen JF, Troost D, van der Kracht AH, Wondergem J, Haveman J, Gonzalez D. Ultrastructural changes in the rat sciatic nerve after local hyperthermia. *Int J Hyperthermia* 1993; 9: 723–30.
28. Meshorer A, Prionas SD, Fajardo LF, Meger JL, Hahn GM, Martinez AA. The effects of hyperthermia on normal mesenchymal tissues. *Arch Pathol Lab Med* 1983; 107: 328–34.
29. Toglia A, Roemer RB, Kittleson J, Carter P, Hodak J. Cerebral bloodflow in and around spontaneous malignant gliomas. *Int J Hyperthermia* 1996; 12: 461–76.
30. Wan H, Aarsvold J, O'Donnell M, Cain CA. Thermal dose optimization for ultrasound tissue ablation. *IEEE Trans UFFC* 1999; 46: 913–28.
31. Dorr LN, Hynynen K. The effects of tissue heterogeneities and large blood vessels on the thermal exposure induced by short high-power ultrasound pulses. *Int J Hyperthermia* 1992; 8: 45–59.
32. Hutchinson EB, Hynynen K. Intracavitary ultrasound phased arrays for prostate thermal therapies: MRI compatibility and *in vivo* testing. *Med Phys* 1998; 12: 2392–9.
33. Hynynen K, Vykhodtseva NI, Chung AH, Sorrentino V, Colucci V, Jolesz FA. Thermal effects of focused ultrasound on the brain: determination with MR imaging. *Radiology* 1997; 204: 247–53.
34. Anhalt DP, Hynynen K, Roemer RB. Patterns of changes of tumour temperatures during clinical hyperthermia: implications for treatment planning, evaluation and control. *Int J Hyperthermia* 1995; 11: 425–36.
35. Arora D, Skliar M, Roemer RB. Model predictive control of hyperthermia treatments. *IEEE Trans Biomed Eng* 2002; 49: 629–39.